Microcalorimetric and Infrared Studies of Ethanol and Acetaldehyde Adsorption to Investigate the Ethanol Steam Reforming on Supported Cobalt Catalysts

José M. Guil,*,† Narcís Homs,‡ Jordi Llorca,‡ and Pilar Ramírez de la Piscina*,‡

Instituto de Química Física "Rocasolano", CSIC, Serrano 119, 28006 Madrid, Spain, and Departament de Química Inorgànica, Universitat de Barcelona, Martí i Franquès 1-11, 08028 Barcelona, Spain

Received: January 24, 2005; In Final Form: March 8, 2005

Microcalorimetric and infrared studies of ethanol and acetaldehyde adsorption were carried out on fresh and deactivated ZnO-supported cobalt catalysts (Co/ZnO and Co/ZnO(d), respectively) as well as on ZnO support alone. The results were used to analyze the catalytic behavior of these materials for ethanol and acetaldehyde steam-reforming reactions. The Co/ZnO(d) sample contained extensive carbon deposition as shown by Raman spectroscopy and transmission electron microscopy. On fresh Co/ZnO, the adsorption energetics of ethanol and acetaldehyde (an intermediate in the ethanol reforming reaction) were similar. Under steam-reforming conditions at low conversion values of ethanol, acetaldehyde was selectively yielded. The presence of surface acetate species was shown from IR spectra following acetaldehyde adsorption. Besides that, the Co/ZnO catalyst was active and showed a high selectivity toward the reforming products, H_2 and CO_2, when the steam reforming of acetaldehyde was carried out at low conversion values. In contrast, on the deactivated sample, the strongest adsorption sites of ethanol have disappeared, and acetaldehyde was adsorbed with higher energy with respect to ethanol, resulting in the blockage of the active sites; a poorer catalytic performance in both ethanol and acetaldehyde steam-reforming reactions is observed. The presence of acetate species after adsorption of acetaldehyde on Co/ZnO(d) was not shown. The polymerization of acetaldehyde over Co/ZnO-(d) was related to the decomposition of acetaldehyde under reforming conditions to give CO and CH_4.

Introduction

There is a growing interest in the sustainable production of hydrogen from renewable sources for energy applications, such as fuel cells. In recent years, one of the substrate of interest has been ethanol, since it can be obtained from biomass and it is easy and safe to manipulate. The steam reforming of ethanol

$$C_2H_5OH + 3H_2O \rightarrow 6H_2 + 2CO_2$$

can yield up to 6 mol of H_2 per mol of reacted ethanol, and global CO_2 emission can be considered neutral. It is a complex process that has been studied from different points of view and over several catalytic systems.[1−20] Over cobalt-based systems, it has been shown that the first step is the dehydrogenation of ethanol to acetaldehyde, after which acetaldehyde is reformed.[18,21] Several nondesired reactions can occur under the steam-reforming conditions; consequently, products other than hydrogen and CO_2 are usually obtained. Besides the low selectivity, the deposition of carbon has been reported as a major problem for the process.[4−6,10,11,16,18−20] The study of the energetics of the interaction of ethanol and acetaldehyde, which is the intermediate product, with the surface of the fresh and deactivated catalyst, can help to ameliorate our knowledge of the reaction and the reasons for deactivation. In this context, it is well-known that the energetics of the interaction of reactants and products with the surface of a catalyst condition its activity and selectivity and that usually deactivation leads to a change in the selectivity of the catalyst. Often, if the adsorption of the reactant is weak, then an increase of the reaction rate with the heat of adsorption is observed as a consequence of the increase of the surface coverage, and a maximum rate is reached for an optimum surface coverage. Then, an increase in the strength of adsorption produces a decrease in the reaction rate. For consecutive reactions, the strong adsorption of one of the products of an initial step can also block the active sites, slowing down the total process.[22]

The present paper is addressed to the study of ethanol steam reforming in terms of understanding the catalyst deactivation phenomena. These phenomena are analyzed in the light of the changes in magnitude of the interaction of reactants and products with the surface of fresh and deactivated catalyst.

The catalytic behavior on ethanol and acetaldehyde steam reforming of fresh and deactivated Co/ZnO catalysts was determined under low conversion values. Differences in the catalytic behavior of the support, fresh, and deactivated samples were examined in the light of microcalorimetric and infrared studies of adsorption of ethanol and acetaldehyde.

Experimental Section

Preparation of Catalysts. Three samples were prepared and studied, pure ZnO and two ZnO-supported cobalt samples (fresh and deactivated). The ZnO support was prepared by decomposition of $3ZnO{\cdot}2ZnCO_3{\cdot}3H_2O$ under Ar at 573 K. The preparation of ZnO-supported cobalt catalyst (labeled as Co/ZnO) has already been reported.[15] Co/ZnO was prepared by the incipient wetness method with an aqueous solution of $Co(NO_3)_2$. After impregnation, the sample was dried at 373 K, calcined at 673 K, and reduced under H_2 at 673 K. The cobalt content was 9.4

* Author to whom correspondence should be addressed. Phone: 34 91 5619400 (J.M.G.); 34 93 4037056 (P.R.P.). Fax: 34 91 5642431 (J.M.G.); 34 934907725 (P.R.P). E-mail: rocguil@iqfr.csic.es; pilar.piscina@qi.ub.es.
† Instituto de Química Física "Rocasolano", CSIC.
‡ Departament de Química Inorgànica, Universitat de Barcelona.

10.1021/jp050414k CCC: $30.25
Published on Web 05/06/2005

wt % as determined by inductively coupled plasma atomic absorption. Deactivated Co/ZnO (labeled as Co/ZnO(d)) was prepared by treating Co/ZnO under a C_2H_5OH/H_2O/Ar mixture of 1:3:2 (molar basis) at 723 K and a gas hourly space velocity (GHSV) of 5000 h^{-1} for 48 h. At the end of the treatment, the flow of $C_2H_5OH + H_2O$ was stopped, and the sample was cooled under Ar stream and stored for study.

Catalytic Tests. The catalytic studies were carried out in a continuous flow glass microreactor at atmospheric pressure. Temperature was increased from 598 to 623 K. To avoid significant deactivation (for Co/ZnO) or additional deactivation (for Co/ZnO(d)) of samples during the acquisition of data, the total time of the catalytic studies was kept under 4.5 h. Different amounts of catalysts (300−500 mg for ZnO and 30−100 mg for Co/ZnO and Co/ZnO(d)) were used to attain similar conversion values (lower than 20%) under the same experimental conditions. Catalysts were diluted with inactive SiC to operate at a GHSV of 10^4 h^{-1}. The reagent feed was either a gaseous mixture of ethanol and water diluted in argon (C_2H_5OH/H_2O/Ar = 1:3:20 molar ratio) or a gaseous mixture of acetaldehyde and water diluted in argon (CH_3CHO/H_2O/Ar = 1:3:20 molar ratio). A constant mixture of liquid (HPLC purity grade) was supplied by a Gilson 307 piston pump, vaporized at 453 K, and then mixed with the Ar flow before entering the reaction chamber. The catalyst was first heated to 573 K under Ar, then the reactant mixture was introduced, and the temperature was increased to the reaction temperature (598−623 K). Products were analyzed inline by gas chromatography as described elsewhere.[4] The detection limit of CO was ca. 20 ppm. Response factors for all products were obtained with appropriate standards before and after each catalytic test.

Catalyst Characterization. Infrared experiments were carried out on pelleted samples that were treated in situ by successive hydrogen/vacuum cycles at 673 K. Infrared spectra were obtained at room temperature on a Nicolet 520 Fourier transform instrument at a resolution of 2 cm^{-1} by collecting 256 scans. Greaseless cells that allowed thermal and vacuum treatments equipped with CaF_2 windows were used. Adsorption of acetaldehyde was accomplished by means of vacuum-gas-line techniques.

Raman spectroscopy was performed with a Jobin Yvon T64000 instrument using an Ar ion laser as an illumination source (514.5 nm) and a CCD detector cooled to 140 K. The Raman instrument was coupled to a standard Olympus microscope (×50 magnification), and the collection optics system was used in the backscattering configuration. The laser power at the sample was limited to 3 mW to prevent heating.

Conventional transmission electron microscopy and high-resolution transmission electron microscopy (HRTEM) was performed on a Philips CM-30 instrument equipped with a LaB_6 source and operating at 300 kV, with a point-to-point resolution of 0.19 nm. Samples were deposited on copper grids with a holey-carbon-film support. Magnification and camera constants were calibrated using appropriate standards in the same electron-optical conditions.

Adsorption Microcalorimetry. Adsorption measurements were performed in a Tian-Calvet heat-flow microcalorimeter (model BT, Setaram, France) coupled to a conventional volumetric apparatus as described in detail elsewhere.[23]

Calibration of the heat/voltage constant of the microcalorimeter was accomplished by the Joule effect. The correction for the heat evolved in the gas compression associated with the gas entrance to the cell was determined by previous experiments with helium. In that way, the differential isosteric heat of adsorption was determined.[24] Reproducibility of the calorimetric measurements, estimated from the mean deviation of a series of helium expansion experiments, was on the order of 2 mJ.

Dead volumes of the coupled volumetric apparatus were carefully calibrated either by mercury weighing or by helium expansions. This, together with the use of a capacitance manometer (Baratron 310, MKS), ensured a high degree of precision in determining the amount adsorbed. Reproducibility, measured by cumulative helium expansions, was always better than 0.2 μmol.

Through the measurement of the amounts adsorbed at increasing pressures and the heat evolved in the adsorption of each one of the subsequent doses of the adsorbate, the volumetric isotherms, $n^{ads}-p$, and differential calorimetric isotherms, $q^{ads}-n^{ads}$, were simultaneously obtained.[23]

Readsorption experiments were performed after outgassing (10^{-5} mbar) for a period of 30 min at the temperature of the experiment. The amount desorbed in this process was determined from the calorimetric desorption peak. From this, the amount remaining irreversibly adsorbed was calculated. If the readsorption isotherm is displaced by that amount to the right-hand side, it overlaps with the final part of the adsorption isotherm, thus confirming that the readsorption experiment simply replaces the reversible amount removed by outgassing.

Results and Discussion

The catalytic behavior of the ZnO and Co/ZnO samples in the ethanol steam-reforming reaction under high conversion values and low C_2H_5OH/H_2O ratio (1:13 molar, a bioethanol-like mixture) has already been reported.[1,15] Although ZnO has been shown to be active, the introduction of cobalt produces a catalyst with a much better performance for hydrogen production. The catalytic capability of ZnO has been related to its basic and redox properties.[1] For ZnO-supported cobalt catalysts, oxidized cobalt and metallic cobalt coexist on the surface during the reaction, and they contribute to the global performance of the catalyst.[14,15]

On both catalysts, ZnO and Co/ZnO, the generation of carbonaceous residues after reaction has been shown.[15] To highlight the differences between catalysts, these were studied under reforming conditions of ethanol at low conversion values and stoichiometric C_2H_5OH/H_2O ratios (1:3 molar). Moreover, the Co/ZnO catalyst was deliberately deactivated, giving the Co/ZnO(d) sample, which was also tested and characterized. Figure 1 shows transmission electron micrographs corresponding to Co/ZnO(d). Cobalt particles of ca. 10 nm covered by carbonaceous deposits are distributed over the surface of the sample; in some cases these particles are located inside carbon filaments (Figure 1a). A high-resolution image corresponding to a single metallic cobalt particle surrounded by a poorly ordered carbonaceous phase (C(002) at 3.7 Å) with an onion-shell-type structure is shown in Figure 1b. Figure 2 displays the Raman spectrum in the range 1200−1700 cm^{-1} for the deactivated sample. Two broad bands centered at 1334 and 1592 cm^{-1} are observed, and these are characteristic of disordered carbon materials.[25,26] The Raman spectra of single crystals of graphite only show one band corresponding to the E_{2g} mode around 1575 cm^{-1}, the only Raman-active mode of an infinite crystal. This band shifts toward higher wavenumbers with extremely small crystallites. However, polycrystalline graphite exhibits another band around 1355 cm^{-1}. This has been attributed to an A_{1g} mode of the lattice that becomes Raman-active due to the finite crystal size. The intensity of this band has been demonstrated to be inversely proportional to the

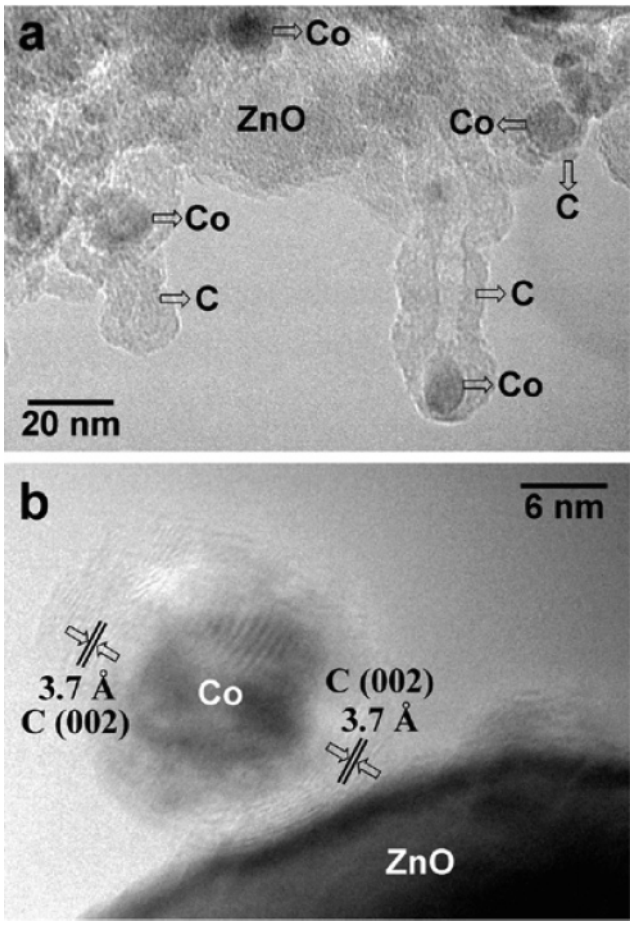

Figure 1. Transmission electron microscopy images corresponding to the deactivated sample, Co/ZnO(d).

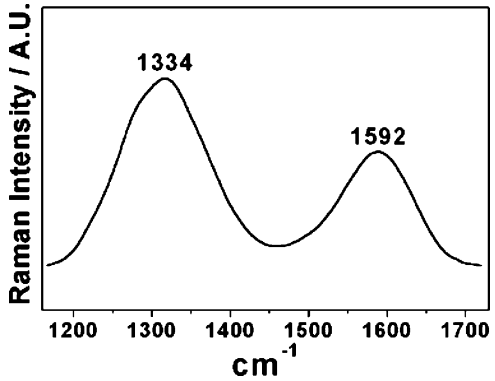

Figure 2. Raman spectrum in the carbon region of the deactivated sample, Co/ZnO(d).

effective crystallite size in the direction of the graphite plane, so that the band allows the measurement of the crystallite size in a thin surface layer of any carbon sample.[25,26] For Co/ZnO-(d), the calculated microcrystalline planar size ($L = 44(I_{1592}/I_{1334})$ is ca. 2 nm, a size which is in accordance with the TEM measurements (Figure 1b).

The catalytic behavior of the samples under a $C_2H_5OH/H_2O/Ar = 1:3:20$ mixture is compiled in Table 1. As stated in the Experimental Section, to attain similar conversion values, different sample amounts were used to carry out the catalytic tests. At similar conversion values and reaction temperatures, the activity of Co/ZnO is ca. 10-fold that of ZnO, the activity of Co/ZnO(d) always being well below than that of Co/ZnO. Over Co/ZnO and Co/ZnO(d), the predominant reaction was the dehydrogenation of ethanol to acetaldehyde, which is an intermediate product in the ethanol steam reforming over these systems.[18,21] According to the stoichiometry of the reaction

$$C_2H_5OH \rightarrow CH_3CHO + H_2$$

similar amounts of acetaldehyde and hydrogen evolved over the ZnO-supported cobalt samples, whereas only minor amounts of CO and CH_4 were produced. Over Co/ZnO(d), the selectivity to CH_4, although very low, is higher than that attained over Co/ZnO. For Co/ZnO and Co/ZnO(d), selectivity does not change significantly with the conversion, at least up to ca. 18% of the ethanol conversion values.

Over ZnO, in addition to the dehydrogenation of ethanol, 10−36% of the ethanol reacted producing dimethyl ketone, and 20−25% of ethanol dehydrated to ethylene. Although alcohols can evolve over ZnO giving both dehydrogenation or dehydration reactions, the first process is usually favored.[27] Dimethyl ketone can be produced, over the basic centers of ZnO, from the aldolic condensation of acetaldehyde to butan-1-al-3-ol and further dehydrogenation and cleavage reactions.[28] The selectivity to dimethyl ketone increased, and that to acetaldehyde decreased when conversion increased, which indicates that dimethyl ketone formed from the acetaldehyde produced in the first step of the reaction.

Taking into account that acetaldehyde appears as an intermediate in the ethanol steam reforming on these catalysts, they were tested with an acetaldehyde feed under steam-reforming conditions. Results are shown in Table 2. Over ZnO, mainly dimethyl ketone was produced, and only a minor ratio of acetaldehyde was decomposed to CO and CH_4 or reformed to H_2 and CO_2. The selectivity pattern was in good agreement with a global process

$$2CH_3CHO + H_2O \rightarrow 2H_2 + CO_2 + CH_3COCH_3$$

The catalytic behavior of Co/ZnO(d) under a $CH_3CHO/H_2O = 1:3$ molar mixture differed from that of the fresh sample, Co/ZnO. Steam reforming of acetaldehyde was mainly produced on Co/ZnO

$$CH_3CHO + 3H_2O \rightarrow 5H_2 + 2CO_2$$

In contrast, the selectivity values to CO and CH_4 obtained over Co/ZnO(d) indicated that the main reaction over Co/ZnO(d) was acetaldehyde decomposition

$$CH_3CHO \rightarrow CH_4 + CO$$

This represents quite a different evolution of the intermediate acetaldehyde on both samples. To understand this reaction pathway, a study of the interaction of both ethanol and acetaldehyde was carried out by means of microcalorimetry and infrared spectroscopy.

As is well-known, the energetics of the interaction of reactants, intermediates, and products with the surface active sites conditions the catalyst activity and selectivity. Figures 3−6 show the differential heats of ethanol and acetaldehyde adsorption, q^{ads}, on the three samples, as a function of the amount adsorbed, n^{ads}.

On Co/ZnO, calorimetric curves, $q^{ads}-n^{ads}$, of similar shape are found for both adsorbates (Figure 3). This indicates that the adsorption sites are likely the same. High adsorption heats are found at low and medium coverages similar to those published in the literature for the same adsorbates on Cu/SiO_2.[29] The differential heat of adsorption of ethanol and acetaldehyde

TABLE 1: Catalytic Behavior in the Ethanol Steam-Reforming Reaction[a]

catalyst	T (K)	activity (mmol C_2H_5OH/(g of catalyst h))[c]	conversion C_2H_5OH (%)	selectivity[b] (%)						
				H_2	CO_2	CO	CH_4	C_2H_4	CH_3CHO	CH_3COCH_3
ZnO	598	0.25	4.7	45.4				11.3	40.4	2.9
Co/ZnO	598	2.19	4.1	49.4			0.5	0.3	49.8	
Co/ZnO(d)	598	1.56	5.4	48.1			1.8		50.1	
ZnO	610	0.86	9.7	46.2	5.3			11.9	29.9	6.7
Co/ZnO	610	8.02	9.0	49.6			0.5	0.4	49.5	
Co/ZnO(d)	598	1.52	10.5	48.2			1.8		50.0	
ZnO	623	0.85	15.9	51.0	7.4			12.7	19.8	9.1
Co/ZnO	623	9.03	16.9	50.4		1.6	0.9	0.1	47.0	
Co/ZnO(d)	623	2.54	17.5	48.7		0.4	1.6		49.3	

[a] Reaction conditions: total pressure, 1 atm; $C_2H_5OH/H_2O/Ar = 1:3:20$ (molar ratio); GHSV= 10 000 h^{-1}; catalyst amount 30−500 mg. [b] Water not included. [c] For Co/ZnO(d), grams of catalyst refers to the mass of catalyst before the deactivation treatment (carbon excluded).

TABLE 2: Catalytic Behavior in the Acetaldehyde Steam-Reforming Reaction[a]

catalyst	T (K)	activity (mmol CH_3CHO/(g of catalyst h))[c]	conversion CH_3CHO (%)	selectivity[b] (%)				
				H_2	CO_2	CO	CH_4	CH_3COCH_3
ZnO	598	0.11	1.2	51.9	24.8		0.1	23.2
Co/ZnO	598	0.16	0.6	60.5	24.7	9.9	4.9	
Co/ZnO(d)	598	0.08	1.0	24.6	19.8	25.3	30.3	
ZnO	610	0.40	7.4	52.0	25.4		0.2	23.6
Co/ZnO	610	3.18	8.2	61.8	25.8	9.1	3.3	
ZnO	623	1.01	11.1	51.9	24.2		0.3	23.6
Co/ZnO	623	4.62	11.9	62.4	26.6	8.6	2.4	
Co/ZnO(d)	623	0.76	10.3	27.2	24.9	19.2	28.7	

[a] Reaction conditions: total pressure, 1 atm; $CH_3CHO/H_2O/Ar = 1:3:20$ (molar ratio); GHSV= 10 000 h^{-1}; catalyst amount 30−500 mg. [b] Water not included. [c] For Co/ZnO(d), grams of catalyst refers to the mass of catalyst before the deactivation treatment (carbon excluded).

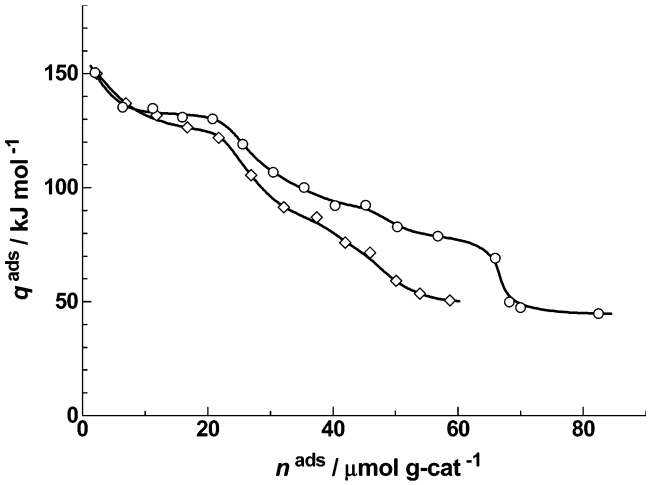

Figure 3. Differential heat of adsorption of ethanol and acetaldehyde on Co/ZnO catalyst at 315 K as a function of amount adsorbed: ◇, ethanol; ○, acetaldehyde.

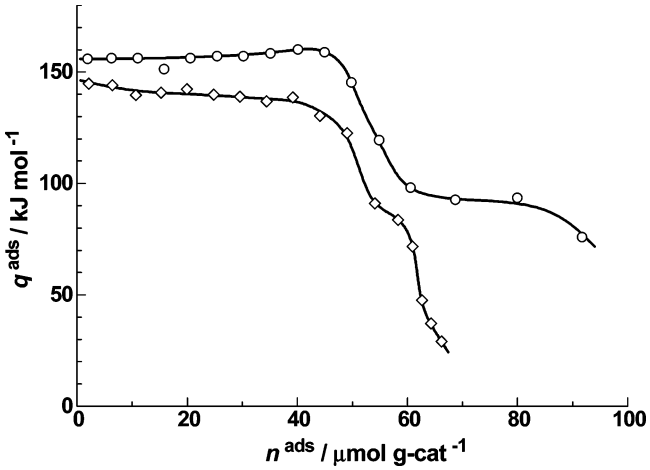

Figure 4. Differential heat of adsorption of ethanol and acetaldehyde on ZnO catalyst at 315 K as a function of amount adsorbed: ◇, ethanol; ○, acetaldehyde.

are equal at very low coverage (0−8.5 μmol g^{-1} of catalyst) (Figure 3). At higher coverage, the adsorption heat of ethanol was only somewhat lower than that of acetaldehyde. Taking into account the adsorption energetics of reactants and products, this is a proper situation for a high catalytic activity; the time of residence of both adsorbates in the most energetic sites is similar, and once an ethanol molecule is adsorbed, it can be activated, and there is a certain probability that the reaction will take place. In contrast, ZnO exhibited many sites for ethanol adsorption of high energy (Figure 4), similar to that of the strongest sites of Co/ZnO (Figure 3).[30] However, on ZnO acetaldehyde is adsorbed on the same sites, as shown by the similar shape of the calorimetric curves of the two adsorbates, with higher energy. This may result in the blockage of the active sites, explaining the lower activity of ZnO with respect to Co/ZnO under ethanol steam-reforming conditions (Table 1).

The different interactions of ethanol and acetaldehyde with ZnO and Co/ZnO were also reflected in the different selectivities of both catalysts under ethanol and acetaldehyde steam-reforming conditions. As indicated above, the production of dimethyl ketone can be related to the interaction of acetaldehyde with the basic centers of ZnO.[1] These centers are not present on the Co/ZnO catalyst (compare the difference of shape between the calorimetric curves of the two samples, Figures 3 and 4).

However, the calorimetric curves of ethanol and acetaldehyde on the deactivated sample, Co/ZnO(d), show important differences when compared with those on Co/ZnO. The $q^{ads}-n^{ads}$ curves of ethanol adsorption on the two samples are plotted in Figure 5. Both curves run parallel, the heats of adsorption being lower on the deactivated sample. If the curve of Co/ZnO(d) is displaced 5.5 μmol g^{-1} of catalyst to the right-hand side, both curves coincide at high adsorption heats (140−90 kJ mol^{-1})

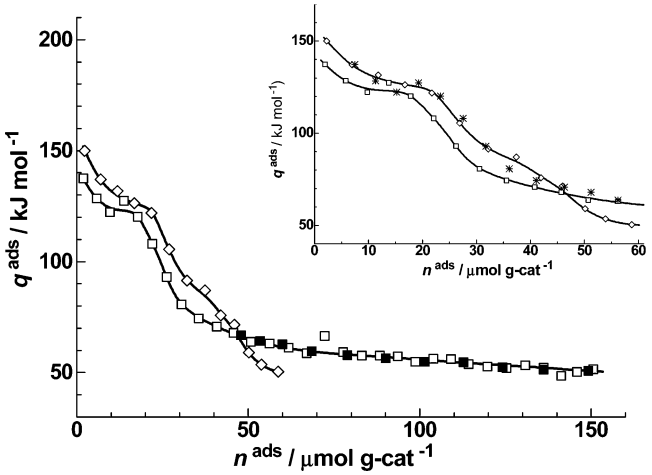

Figure 5. Differential heat of adsorption of ethanol on Co/ZnO and Co/ZnO(d) catalysts at 315 K as a function of amount adsorbed: ◇, Co/ZnO; □, Co/ZnO(d); ■, readsorption on Co/ZnO(d), displaced 45 μmol g^{-1} of catalyst to the right-hand side (Experimental Section). Inset: Adsorption (∗) on Co/ZnO(d) displaced 5.5 μmol g^{-1} of catalyst to the right-hand side (see text).

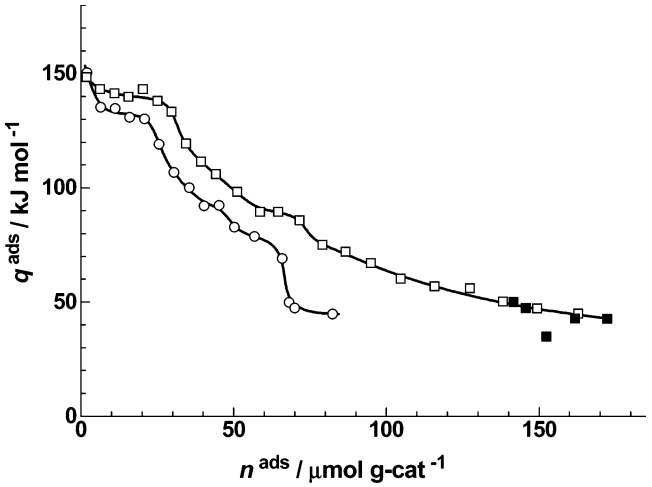

Figure 6. Differential heat of adsorption of acetaldehyde on Co/ZnO and Co/ZnO(d) catalysts at 315 K as a function of amount adsorbed: ○, Co/ZnO; □, Co/ZnO(d); ■, readsorption on Co/ZnO(d), displaced 140 μmol g^{-1} of catalyst to the right-hand side (Experimental Section).

(see inset in Figure 5). This indicates that only a small fraction of the most energetic active sites (5.5 μmol g^{-1} of catalyst) has disappeared in the deactivated sample with respect to the fresh sample. The higher activity of the Co/ZnO sample can be ascribed to those few more energetic sites. The disappearance of these sites upon deactivation explains the lower catalytic activity of Co/ZnO(d). In addition, the heats of adsorption of acetaldehyde on Co/ZnO(d) increased relative to the values on the fresh sample (Figure 6). The adsorption heats of acetaldehyde on Co/ZnO(d) are even above the adsorption heats of ethanol. This is an additional explanation for the strong lowering of the catalytic activity of the deactivated sample, by blockage of the active sites with acetaldehyde.

Another remarkable feature of the adsorption on Co/ZnO(d) is the much higher uptakes of both adsorbates but with lower heats (Figures 5 and 6). The deposition of carbonaceous residues upon deactivation, as unveiled above by TEM and Raman spectroscopy results, produces an increase of the specific surface area of Co/ZnO(d). The adsorption heats in the extended zone, 60−80 to 160−180 μmol g^{-1} of catalyst, lay in the range of 70−40 kJ mol^{-1} (Figures 5 and 6), and these are values similar to those found for acetaldehyde adsorption on activated carbons.[31,32] Below that coverage range, heats of acetaldehyde adsorption are higher. High values of acetaldehyde adsorption on silica were ascribed to oligomerization processes.[33] Furthermore, readsorption experiments carried out after 30 min of outgassing at the temperature of the experiment, 315 K, (full symbols in Figures 5 and 6) yielded significantly different amounts irreversibly adsorbed, 45 and 140 μmol g^{-1} of catalyst for ethanol and acetaldehyde on Co/ZnO(d), respectively. The oligomerization product with multiple bonds to the surface can account for the large amount of acetaldehyde that remains on the surface after outgassing. The different interaction of acetaldehyde with Co/ZnO and Co/ZnO(d) probably conditions their different selectivity under acetaldehyde steam-reforming conditions. The major reaction over Co/ZnO was the reforming of acetaldehyde, while over Co/ZnO(d) the major reaction was its decomposition (Tables 1 and 2).

To investigate the nature of the resulting surface species and relate them to the catalytic and microcalorimetric results, acetaldehyde adsorption on fresh and deactivated catalysts was followed by FTIR. Figure 7 shows the spectra corresponding to the Co/ZnO sample. The initial interaction produced surface acetate species, characterized by two broad bands centered at 1580 and 1435 cm^{-1}, which correspond to υ_{asym}(COO) and υ_{sym}(COO), respectively.[34,35] Additional small bands due to surface acetate were found at 1348 cm^{-1} (δ(CH$_3$)), 1052 and 1029 cm^{-1} (ρ(CH$_3$)), 2997 cm^{-1} (υ_{asym}(CH$_3$)), and 2939 cm^{-1} (υ_{sym}(CH$_3$)). All of these bands disappeared after a treatment under vacuum at 573 K (Figure 7, spectra a−d). A second exposition of the sample to acetaldehyde produced the appearance of similar bands characteristic of surface acetate species and other minor bands in the zone 1200−900 cm^{-1} and in the υ(CH) zone (Figure 7, spectra e−f). The latest bands highly diminished with a vacuum treatment at room temperature and disappeared completely after a vacuum treatment at 323 K. The existence of surface acetate species resulting from acetaldehyde adsorption has been detected on different systems, such as ZnO,[34] oxidized Rh(111),[36] and oxidized Ag(111).[37,38] In the latter case, the adsorption of acetaldehyde produced polyacetaldehyde and ethane-1,1-dioxy surface intermediates that ended in stable acetate species bidentate-bridged to the surface.

When acetaldehyde adsorption was carried out on Co/ZnO(d), no bands assigned to acetate species emerged (Figure 8), and only small bands in the zone 1460−990 cm^{-1} and in the υ(CH) region appeared. These bands diminished after a high vacuum treatment at room temperature. They can be assigned to polyacetaldehyde species:[37,39] ∼1420 cm^{-1} (δ_{asym}(CH$_3$)), 1348 cm^{-1} (δ_{sym}(CH$_3$)), 1185 cm^{-1} (υ_{asym}(OCO)), 1106 cm^{-1} (υ_{sym}(OCO)), and ∼950 cm^{-1} (ρ(CH$_3$)). The comparison between spectrum a in Figure 8 and spectrum e in Figure 7 shows that these species were also formed after the second exposition of acetaldehyde on Co/ZnO. IR experiments point out that on the deactivated sample polymerization of acetaldehyde takes place and remains on the surface without further transformation. Acetaldehyde polymerization is an exothermic process that causes the higher heat of acetaldehyde adsorption measured on the deactivated sample. Multiple bonds to the surface may be formed and result in a large amount of irreversibly adsorbed acetaldehyde, as determined from microcalorimetric experiments (Figure 6). Moreover, adsorbed polymerized acetaldehyde would easily decompose under vacuum, generating adsorbed species that prevent the interaction of acetaldehyde with the initial adsorption centers; these adsorbed species could not be detected by IR. The formation of different surface species from acetal-

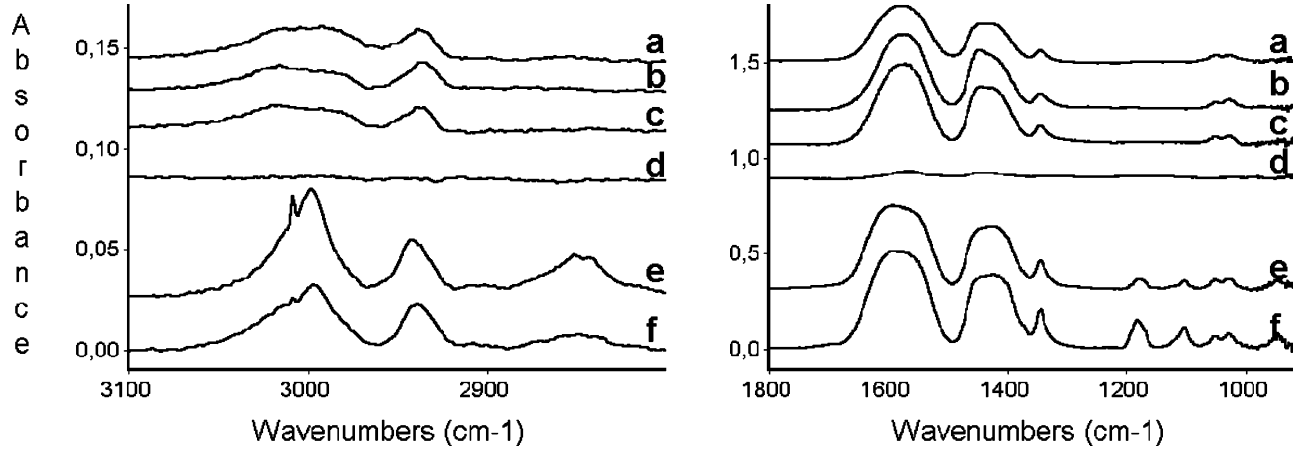

Figure 7. FTIR spectra of acetaldehyde adsorption on Co/ZnO after successive vacuum treatments, 5 min at 5×10^{-5} mbar at different temperatures: (a) room temperature; (b) 323 K; (c) 423 K; (d) 573 K. (e) Readsorption of acetaldehyde after experiment (d) followed by vacuum treatment (5 min, room temperature, 4×10^{-3} mbar); (f) vacuum treatment (room temperature, 6×10^{-4} mbar) after experiment (e).

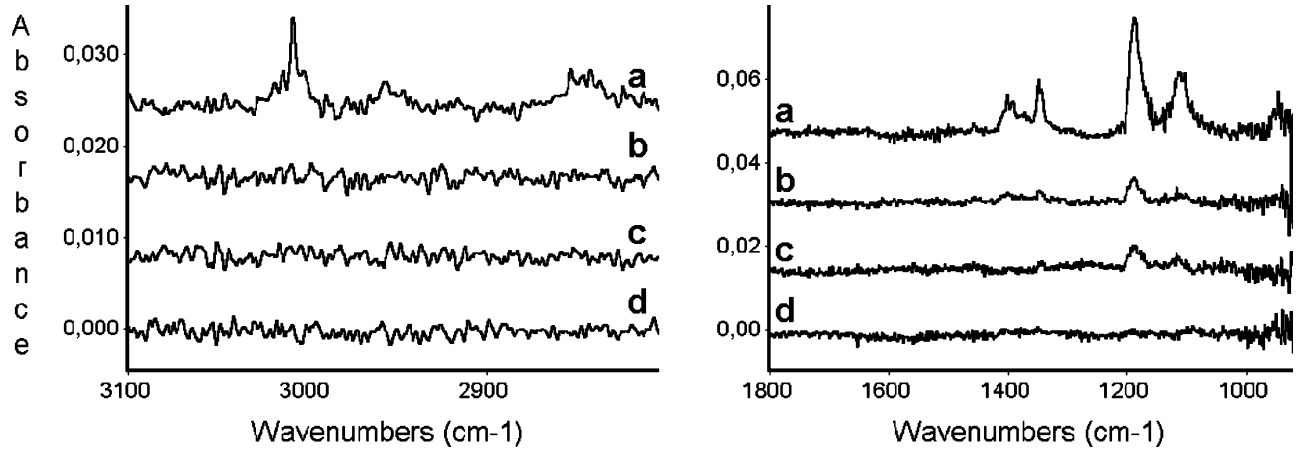

Figure 8. FTIR spectra of acetaldehyde adsorption on Co/ZnO(d) after successive vacuum treatments (5 min): (a) 4×10^{-3} mbar at room temperature; (b) 6×10^{-4} mbar at room temperature; (c) 10^{-5} mbar at room temperature; (d) 10^{-5} mbar at 323 K.

dehyde adsorption on oxidized Ag(111) as a function of temperature has been described (140−220 K).[37] At 140 K, the formation of polyacetaldehyde takes place, which transforms to acetate at 220 K. Moreover, the disappearance of acetate bands occurred at ∼450 K without detecting spectroscopically any surface species either. In our case, the different interaction of acetaldehyde with the active sites of the fresh and deactivated samples can condition the selectivity to reforming or decomposition of acetaldehyde as well as the lower catalytic activity of the deactivated sample when it is compared to that of the fresh catalyst. These results accord with in situ diffuse reflectance IR Fourier transform studies of steam reforming of ethanol over Co/ZnO catalysts carried out previously.[21] It has been shown that the C−C scission of surface acetate species on cobalt is related to the H_2 production in the steam-reforming reaction of ethanol.

Conclusions

The combination of microcalorimetric and infrared spectroscopic studies has been demonstrated to be an efficient and powerful approach for the understanding of ethanol and acetaldehyde adsorption on ZnO and ZnO-supported cobalt catalysts and their subsequent transformation under steam-reforming conditions. The accumulation of carbonaceous residues during ethanol steam reforming over Co/ZnO has a strong effect on the catalyst performance, which is reflected by a lower ethanol and acetaldehyde conversion under steam-reforming conditions. Moreover, a significant change in product selectivity for acetaldehyde steam reforming is found. Over Co/ZnO, H_2 and CO_2 are selectively produced, but Co/ZnO(d) favors acetaldehyde decomposition to CH_4 and CO. This catalytic behavior is well-explained by the energetics of the interaction of both ethanol and acetaldehyde with the surface active sites of Co/ZnO and Co/ZnO(d). On the deactivated sample, most energetic adsorption sites of ethanol disappear with respect to the fresh catalyst. In addition, the heats of acetaldehyde adsorption on the deactivated sample increase relative to the fresh catalyst and are well above the heats of ethanol adsorption. As a result, the blockage of the active sites by acetaldehyde takes place. This adsorption heat increase is related to acetaldehyde polymerization, as revealed by infrared spectroscopy. This is related to the acetaldehyde decomposition under steam-reforming conditions. In contrast, on the fresh catalyst adsorbed acetaldehyde transforms to acetate surface species. Under steam-reforming conditions, these species produce the desired reforming products, H_2 and CO_2.

Acknowledgment. We thank MCYT (MAT 2002-01739) and CIRIT (2001SGR-00052) for financial support. J.Ll. is grateful to MCYT for a Ramon y Cajal research program fellowship and DURSI (Generalitat de Catalunya).

References and Notes

(1) Llorca, J.; Ramírez de la Piscina, P.; Sales, J.; Homs, N. *Chem. Commun.* **2001**, 641.

(2) Fatsikostas, A. N.; Kondarides, D. I.; Verykios, X. E. *Chem. Commun.* **2001**, 851.

(3) Galvita, V. V.; Semin, G. L.; Belyaev, V. D.; Semikolenov, V. A.; Tsiakaras, P.; Sobyanin, V. A. *Appl. Catal., A* **2001**, *220*, 123.

(4) Llorca, J.; Homs, N.; Sales, J.; Ramírez de la Piscina, P. *J. Catal.* **2002**, *209*, 306.

(5) Fierro, V.; Klouz, V.; Akdim, O.; Mirodatos, C. *Catal. Today* **2002**, *75*, 141.

(6) Fatsikostas, A. N.; Kondarides, D. I.; Verykios, X. E. *Catal. Today* **2002**, *75*, 145.

(7) Auprêtre, F.; Descorme, C.; Duprez, D. *Catal. Commun.* **2002**, *3*, 267.

(8) Diagne, C.; Idriss, H.; Kiennemann, A. *Catal. Commun.* **2002**, *3*, 565.

(9) Breen, J. P.; Burch, R.; Coleman, H. M. *Appl. Catal., B* **2002**, *39*, 65.

(10) Freni, S.; Cavallaro, S.; Mondello, N.; Spadaro, L.; Frusteri, F. *Catal. Commun.* **2003**, *4*, 259.

(11) Cavallaro, S.; Chiodo, V.; Freni, S.; Mondello, N.; Frusteri, F. *Appl. Catal, A* **2003**, *249*, 119.

(12) Mariño, F.; Baronetti, G.; Jobbagy, M.; Laborde, M. *Appl. Catal., A* **2003**, *238*, 41.

(13) Liguras, D. K.; Kondarides, I.; Verykios, X. E. *Appl. Catal., B* **2003**, *43*, 345.

(14) Llorca, J.; Dalmon, J. A.; Ramírez de la Piscina, P.; Homs, N. *Appl. Catal., A* **2003**, *243*, 261.

(15) Llorca, J.; Ramírez de la Piscina, P.; Dalmon, J. A.; Sales, J.; Homs, N. *Appl. Catal., B* **2003**, *43*, 355.

(16) Goula, M. A.; Kontou, S. K.; Tsiakaras, P. E. *Appl. Catal., B* **2004**, *49*, 135.

(17) Kaddouri, A.; Mazzocchia, C. *Catal. Commun.* **2004**, *5*, 339.

(18) Llorca, J.; Homs, N.; Sales, J.; Fierro, J. L. G.; Ramírez de la Piscina, P. *J. Catal.* **2004**, *222*, 470.

(19) Frusteri, F.; Freni, S.; Spadaro, L.; Chiodo, V.; Bonura, G.; Donato, S.; Cavallaro, S. *Catal. Commun.* **2004**, *5*, 611.

(20) Frusteri, F.; Freni, S.; Chiodo, V.; Spadaro, L.; Di Blasi, O.; Bonura, G.; Cavallaro, S. *Appl. Catal., A* **2004**, *270*, 1.

(21) Llorca, J.; Homs, N.; Ramírez de la Piscina, P. *J. Catal.* **2004**, *227*, 556.

(22) Kapteijn, F.; Moulijn, J. A.; van Santen, R. A.; Weber, R. Chemical kinetics of catalyzed reactions. In *Catalysis. An Integrated Approach*; van Santen, R. A., van Leeuwen, P. W. N. M., Moulijn, J. A., Averill, B. A., Eds.; Elsevier: Amsterdam, 1999; p 81.

(23) Guil, J. M.; Pérez Masiá, A.; Ruiz Paniego, A.; Trejo Menayo, J. M. *Thermochim. Acta* **1998**, *312*, 115.

(24) Guil, J. M.; Pérez Masiá, A.; Ruiz Paniego, A.; Trejo Menayo, J. M. *J. Chem. Thermodyn.* **1994**, *26*, 5.

(25) Tuinstra, F.; Koenig, J. L. *J. Chem. Phys.* **1970**, *53*, 1126.

(26) Pinheiro, P.; Schouler, M. C.; Gadelle, P.; Mermoux, M.; Dooryhée, E. *Carbon* **2000**, *38*, 1469.

(27) Kung, H. H. *Transition Metal Oxides: Surface Chemistry and Catalysis*; Studies in Surface Science and Catalysis 45; Elsevier: New York, 1989; Chapter 10.

(28) Sreerama Murthy, R.; Patnaik, P.; Sidheswaran, P.; Jayamani, M. *J. Catal.* **1988**, *109*, 298.

(29) Natal-Santiago, M. A.; Sánchez-Castillo, M. A.; Cortright, R. D.; Dumesic, J. A. *J. Catal.* **2000**, *193*, 16.

(30) An experiment of ethanol adsorption on ZnO was carried out at 353 K to check that true equilibrium had been achieved. A $q^{ads}-n^{ads}$ curve similar to that at 315 K was obtained.

(31) El-Sayed, Y.; Bandos, T. J. *J. Colloid Interface Sci.* **2001**, *242*, 44.

(32) El-Sayed, Y.; Bandos, T. J. *Langmuir* **2002**, *18*, 3213.

(33) Natal-Santiago, M. A.; Hill, J. M.; Dumesic, J. A. *J. Mol. Catal. A: Chem.* **1999**, *140*, 199.

(34) Bowker, M.; Houghton, H.; Waugh, K. C. *J. Catal.* **1983**, *79*, 431.

(35) Yee, A.; Morrison, S. J.; Idriss, H. *J. Catal.* **1999**, *186*, 279.

(36) Houtman, C. J.; Brown, N. F.; Barteau, M. A. *J. Catal.* **1994**, *145*, 37.

(37) Sim, W. S.; Gardner, P.; King, D. A. *J. Am. Chem. Soc.* **1996**, *118*, 9953.

(38) Webb, M. J.; Driver, S. M.; King, D. A. *J. Phys. Chem. B* **2004**, *108*, 1955.

(39) Henderson, M. A.; Zhou, Y.; White, J. M. *J. Am. Chem. Soc.* **1989**, *111*, 1185.